ACTA BIOLOGICA CRACOVIENSIA Series Botanica 61/1: 29–42, 2019
DOI: 10.24425/abcsb.2019.127736

Effects of Foliar Application of Cobalt Oxide Nanoparticles on Growth, Photosynthetic Pigments, Oxidative Indicators, Non-Enzymatic Antioxidants and Compatible Osmolytes in Canola (*Brassica napus* L.)

Malihe Jahani[1], Ramazan Ali Khavari-Nejad[1*], Homa Mahmoodzadeh[2] and Sara Saadatmand[1]

[1]*Department of Biology, Science and Research Branch, Islamic Azad University, Tehran, Iran*

[2]*Department of Biology, Mashhad Branch, Islamic Azad University, Mashhad, Iran*

Received February 6, 2019; revision accepted April 9, 2019

Nanotechnology has been widely applied in agriculture, and understanding of the mechanisms of plant interaction with nanoparticles (NPs) as environmental contaminants is important. The aim of this study was to determine the effects of foliar application of cobalt oxide (Co_3O_4) NPs on some morpho-physiological and biochemical changes of canola (*Brassica napus* L.) leaves. Seeds were sown in plastic pots and grown under controlled conditions. Fourteen-day-old seedlings were sprayed with different concentrations of Co_3O_4 NPs (0, 50, 100, 250, 500, 1000, 2000, and 4000 mg L^{-1}) at weekly intervals for 5 weeks. Growth parameters of the shoot (length, fresh and dry weights) were stimulated by low concentrations of Co_3O_4 NPs (50 and 100 mg L^{-1}) and repressed by higher concentrations. Similar trends were observed in photosynthetic pigment contents. The results indicated that high concentrations of Co_3O_4 NPs increased lipoxygenase (LOX) activity and the malondialdehyde (MDA), hydrogen peroxide (H_2O_2), and dehydroascorbate (DHA) contents, but reduced the membrane stability index (MSI), ascorbate (ASC), and glutathione (GSH). Despite the increase of antioxidant capacity (DPPH) and the accumulation of non-enzymatic antioxidants (total flavonoids and flavonols) and osmolytes (proline, glycine betaine (GB) and soluble sugars) at high concentrations of Co_3O_4 NPs, the growth and photosynthesis were reduced. The defence system activity did not seem to be sufficient to detoxify reactive oxygen species (ROS). Altogether, high concentrations of Co_3O_4 NPs showed a phytotoxic potential for canola as an oilseed crop.

Keywords: ascorbate and glutathione, carbohydrate, environmental contaminants, glycine betaine, lipoxygenase activity, total flavonoids and flavonols, toxicity and beneficial assessment

Abbreviations: AFM – atomic force microscopy; ASC – ascorbate; Co_3O_4 NPs – cobalt oxide nanoparticles; DHA – dehydroascorbate; DLS – dynamic light scattering; DPPH – 2,2-diphenyl-1-picrilhydrazil; DW – shoot dry weight; FW – shoot fresh weight; GB – glycine betaine; GSH – glutathione; H_2O_2 – hydrogen peroxide; ICP-OES – inductively coupled plasma optical emission spectrometry; LOX – lipoxygenase; MDA – malondialdehyde; MSI – membrane stability index; ROS – reactive oxygen species; XRD – X-ray diffraction.

INTRODUCTION

During the last few years, nanotechnology has become a powerful technique across different fields including medical, engineering, and agricultural sciences. Several studies have emphasized the importance of nanoparticles (NPs) as a building block for novel applications in plants. The small size of NPs (1-100 nm) and their ability to cross barriers (cell walls and plasma membranes) facilitate effective absorption and modify physicochemical properties compared to the bulk material. Moreover, their large specific surface can result in a good level of interaction with intracellular structures (Ma et al., 2015; Janmohammadi et al., 2017).

* Corresponding author, email: ra.khavarinejad2010@gmail.com

PL ISSN 0001-5296

Different factors such as plant species, NPs type, concentration, chemical composition, surface activity, and size of NPs cause both positive and negative impacts on plant growth, development and metabolism (Rastogi et al., 2017). For instance, the increased seed germination in *Capsicum chinense* imposed by 100–500 mg L^{-1} of ZnO NPs was reported (Garcia-López et al., 2019). Reddy Pullagurala et al. (2018) stated the incremented chlorophyll value in cilantro plants exposed to 400 mg kg^{-1} of nano-ZnO. Furthermore, the increment in chlorophyll index, nodules number and yield in soybean treated with nanometal powders (Co, Fe and Cu) was observed (Ngo et al., 2014). Also, nano Zn-Fe oxide promoted wheat yield under salinity condition (Babaei et al., 2017). In another study, the decrement in seedling growth and chlorophyll content and the increment in reactive oxygen species (ROS) production and DNA damage in *Solanum melongena* exposed to nano-scaled NiO, CuO and ZnO were demonstrated (Baskar et al., 2018). In lettuce imposed by 500–2000 mg L^{-1} of CeO_2 NPs, lipoperoxidation and electrolyte leakage occurred (Cui et al., 2014).

Cobalt (Co) is a magnetic element with properties similar to iron and nickel (Barceloux and Barceloux, 1999). This element plays an essential role in synthesizing several enzymes and coenzymes, symbiotic nitrogen fixation, rhizobia growth, activation of glycolysis enzymes, and oxidizing processes (Sonia and Thukral, 2014). High concentrations of Co have toxic effects on plants including leaf abscission, inhibition of greening and active transport, chlorosis, premature leaf closure, and decrement of dry weight (Sonia and Thukral, 2014).

Owing to their unique physical properties, Co_3O_4 NPs have been applied in pigments, catalysis, sensors, electrochemistry, magnetism, and energy storage (Faisal et al., 2016). In addition, Co_3O_4 NPs are likely to be associated with plants' physiological functions. A previous report on Co_3O_4 NPs (5–20 μg mL^{-1}) demonstrated the reduction of root length in *Allium cepa*, without much elaboration on the nature of cellular damage and the mechanism of phytotoxicity (Ghodake et al., 2011). In *Sesbania cannabina* root meristems exposed to nano-sized cobalt and cobalt oxide, different types of chromosomal aberrations were observed (Srivastava, 2015).

Most previous studies were focused on root or seed exposure and only a few studies reported about the foliar uptake of NPs (Hong et al., 2014; Xiong et al., 2017). In this experiment, due to the use of the foliar spray method, the leaves were directly exposed to NPs treatments as they are the most important and sensitive tissues in this method. In the foliar spray method, the NPs are absorbed through the leaf stomata and cause physio-biochemical changes. Hence, here, leaves were analyzed.

Canola (*Brassica napus* L.) as a member of Brassicaceae family has been known as a healthy and rich source of oil with a low content of saturated fatty acids and high content of polyunsaturated fatty acids (Lin et al., 2013). This plant supplies proteins for feed. In addition, oil seed crops, particularly those containing vitamin E (tocopherol) are thought to demonstrate the high antioxidant capacity and the consumption of food rich in antioxidants provide protection against several diseases (Loganes et al., 2016).

In this study, canola was selected as the test plant because it is one of the most important strategic agricultural products in providing vegetative oil for human consumption. To the best of the authors' knowledge, there is no study on the interaction of Co_3O_4 NPs with canola. Also, in this study, a wide range of concentrations of Co_3O_4 NPs (0–4000 mg L^{-1}) was tested, including high levels; although these concentrations are well above the expected concentrations in the environment, this worst-case scenario allows to better highlight the toxic potential of Co_3O_4 NPs. Furthermore, here, the foliar application way was considered via spraying to leaves. This way as one of the main ways of plant contamination in the environment by NPs is considered (i.e., aerial/rain deposition), allowing a comprehensive and informative picture on the actual impacts of Co_3O_4 NPs contamination towards plant.

Because of the increasing use of nanomaterials such as Co_3O_4 NPs in various commercial and industrial products, releasing these compounds into the environment is predictable. Plants can act as the entry point of NPs into the food chain. Therefore, in this study, the potential beneficial and toxic effects of Co_3O_4 NPs in a wide range of concentrations (0–4000 mg L^{-1}) as foliar spraying on growth, photosynthetic pigments, compatible osmolytes, carbohydrate, oxidative indicators, non-enzymatic antioxidants, antioxidant capacity, and cobalt accumulation in canola were investigated.

MATERIALS AND METHODS

CHARACTERIZATION OF Co_3O_4 NPS

Co_3O_4 NPs were purchased from US Research Nanomaterials, Inc. (Houston, TX, USA). The Co_3O_4 NPs suspension was dispersed using an ultrasonic apparatus (model S.A., FUNGILAB, Barcelona, Spain) at 160 W and 40 Hz for 45 min in deionized water at pH 6.3 and then the surface charge (zeta potential) of NPs was measured by a zeta sizer

(model ZEN3600, Malvern Corp, Worcestershire, UK). Furthermore, the NPs hydrodynamic size was determined based on the dynamic light scattering (DLS) method and using a particle size analyzer (model VASCO 3, Cordouan, Pessac, France) at 25°C. Also, the average size of Co_3O_4 NPs was measured using transmission electron microscopy (TEM; model LEO 912 AB, Zeiss, Oberkochen, Germany) and atomic force microscopy (AFM; model NTEGRA, NT-MDT, Zelenograd, Russia). The structure was assessed using an X-ray diffractometer (XRD; model EXPLORER, GNR, Novara, Italy) at 40 kV and 30 mA.

PLANT MATERIALS AND TREATMENTS

This experiment was performed in a completely randomized design with four replicates. Plastic pots (18 cm height × 19 cm diameter) were filled with a mixture of loam, clay, and sand (2:2:1 ratio) and in each pot, five canola seeds (*Brassica napus* L. cv. Zarfam) were sown at a depth of 2 cm. The pots were placed in a growth chamber with 16/8 h photoperiod, 25 ± 5°C and 30 ± 5% relative humidity. After two weeks, the seedlings were exposed to weekly foliar application of different concentrations of Co_3O_4 NPs (0, 50, 100, 250, 500, 1000, 2000 and 4000 mg L^{-1}) for five times (Supplementary Fig. S1). These concentrations were chosen based on previous studies (Wu et al., 2012; López-Luna et al., 2018). After 50 days, the samples were harvested and the length and fresh and dry weights of the shoots were measured and the leaves were used for physio-biochemical analysis. All chemicals and reagents used in the present study were of analytical grade.

PHOTOSYNTHETIC PIGMENTS (CHLOROPHYLLS AND CAROTENOIDS)

Chlorophyll and carotenoid contents were determined according to the method of Lichtenthaler (1987). Briefly, 0.2 g of fresh leaf samples were extracted with 10 mL of 80% (v/v) acetone and then centrifuged (model 2-6E, Sigma, Osterode, Germany) at 4,000 g for 10 min. The samples were diluted with 80% (v/v) acetone before reading their absorbance at 646.8, 663.2 and 470 nm using a spectrophotometer (model UV-1100, Shimadzu, Kyoto, Japan). The contents of chlorophyll *a*, *b*, total chlorophyll, and carotenoid (mg g^{-1} FW) were calculated using the following equations:

Chlorophyll a = (12.25 $A_{663.2}$ – 2.79 $A_{646.8}$)
Chlorophyll b = (21.50 $A_{646.8}$ – 5.10 $A_{663.2}$)
Total Chlorophyll = Chlorophyll a + Chlorophyll b
Carotenoid = [(1000 A_{470} – 1.82 Chlorophyll a – – 85.02 Chlorophyll b) / 198]

OXIDATIVE INDICATORS (H_2O_2, MALONDIALDEHYDE (MDA), OTHER ALDEHYDES, LIPOXYGENASE (LOX) ENZYME ACTIVITY, AND MEMBRANE STABILITY INDEX (MSI))

H_2O_2 content was measured based on the method described by Velikova et al. (2000). Briefly, 0.5 g of fresh leaf sample was extracted in 0.1% (w/v) trichloroacetic acid (TCA) solution and then the extract was centrifuged at 12,000 g for 15 min. Then, 500 µL of the supernatant was mixed with 500 µL 100 mM potassium phosphate buffer (pH 7) and 2 mL 1 M potassium iodine. The reaction mixture was placed in darkness at room temperature for 1 h before recording the absorbance at 390 nm. The H_2O_2 content (µM g^{-1} FW) was calculated using an extinction coefficient of 0.28 μM^{-1} cm^{-1}.

To measure MDA content, 0.2 g of fresh leaf sample was extracted with 5 mL 0.1% (w/v) TCA and then centrifuged at 10,000 g for 5 min. One mL of the supernatant was mixed with 4 mL 20% (w/v) TCA solution containing 0.5% (w/v) thiobarbituric acid (TBA). The mixture was heated at 95°C for 30 min and then immediately cooled down on ice and centrifuged again at 10,000 g for 10 min. For MDA measurement, the non-specific absorbance of the supernatant at 600 nm was subtracted from the maximum absorbance at 532 nm and an extinction coefficient of 1.55 × 10^5 M^{-1} cm^{-1} was used for calculation (Heath and Packer, 1968). For other aldehydes (propanal, butanal, hexanal, heptanal and propanol dimethyl acetal) measurement, absorbance of 600 nm was subtracted from maximum absorbance of 455 nm and the extinction coefficient of 0.457 × 10^5 M^{-1} cm^{-1} was used for calculation (Miers et al., 1992).

The enzyme activity of LOX (EC 1.13.11.12) was measured based on the method described by Doderer et al. (1992). Initially, the enzyme extract was prepared. Two hundred mg fresh leaf sample was homogenized in an ice-cold mortar using 2 mL of 50 mM potassium phosphate buffer (pH 7.0) containing 1 mM ethylene diamine tetra-acetic acid (EDTA), 1% (w/v) soluble polyvinyl pyrrolidone (PVP) and 1 mM phenyl methane sulfonyl fluoride (PMSF). After centrifugation (VS-15000 CFN P, Vision, Tokyo, Japan) at 20,000 g for 20 min, the supernatant was used as enzyme extract. Then, for measurement of LOX activity, the substrate solution was prepared by adding 35 µL linoleic acid to 5 mL distilled water containing 50 µL Tween-20. The solution was kept at pH 9.0 by adding 0.2 M NaOH until all the linoleic acid was dissolved and the pH remained stable. After adjusting the pH to 6.5 by adding 0.2 M HCl, 0.1 M phosphate buffer (pH 6.5) was added to make a total volume of 100 mL. LOX activity was determined spectrophotometrically

by adding 50 µL of enzyme extract to 2.95 mL substrate. The increase in absorbance at 234 nm was recorded for 5 min at 25°C, and the activity was expressed as produced hydroperoxide (H_2O_2) min^{-1} mg^{-1} protein using an extinction coefficient of 25,000 M^{-1} cm^{-1}.

MSI was determined according to the method of Sairam et al. (1997). First, the fresh leaf samples (0.1 g) were soaked in 10 mL double distilled water. A set of samples was heated at 40°C for 30 min and then electrical conductivity was recorded (C_1). The second set was also heated at 100°C for 10 min in boiling water and then electrical conductivity was recorded (C_2). MSI was calculated according to the following formula:

$$MSI\ (\%) = [1 - (C_1/C_2)] \times 100$$

NON-ENZYMATIC ANTIOXIDANTS (ASCORBATE (ASC), DEHYDROASCORBATE (DHA), GLUTATHIONE (GSH), TOTAL FLAVONOIDS AND FLAVONOLS)

ASC and DHA contents were measured based on the method described by De Pinto et al. (1999). Briefly, total ASC was determined after reduction of DHA to ASC with dithiothreitol (DTT), and the concentration of DHA was estimated from the difference between total ASC pool (ASC + DHA) and ASC. The reaction mixture for total ASC pool contained a 0.1 mL aliquot of the supernatant, 0.25 mL of 150 mM phosphate buffer (pH 7.4), and 0.05 mL of 10 mM DTT. After 10 min at room temperature, 0.05 mL of 0.5% (w/v) N-ethylmaleimide (NEM) was added. ASC was determined in a similar reaction mixture except that 0.1 mL of H_2O was added rather than DTT and NEM. The color was developed in both reaction mixtures after addition of the following reagents: 200 µL of 10% (w/v) TCA, 200 µL of 44% (v/v) orthophosphoric acid, 200 µL of 4% (w/v) α,α'-dipyridyl and 10 µL of 0.3% (w/v) $FeCI_3$. After vortexing, the mixture was incubated at 40°C for 40 min and the absorbance was then read at 525 nm. A standard curve was developed based on ASC. Also, the ASC to DHA ratio was calculated.

GSH content was measured according to the method of Ellman (1959). Briefly, 0.5 g of fresh leaf samples were extracted in 4 mL 15% (w/v) metaphosphoric acid and then the extract was centrifuged at 10,000 g at 4°C for 30 min. Then, 200 µL of the supernatant solution was mixed with 6.2 mL sodium phosphate buffer (pH 7.7) and 200 µL 6 mM 5,5'-dithiobis-(2-nitrobenzoic acid) (DTNB). The mixture was left at room temperature for 30 min before recording the absorbance at 412 nm. GSH content (mg g^{-1} FW) was calculated using a standard curve.

The total flavonoid and flavonol contents were determined according to the aluminium chloride method, described by Akkol et al. (2008). Briefly, the oven-dried and powdered leaf samples (0.1 g) were extracted in 5 mL 80% (v/v) methanol and then 1 mL of the extract was mixed with 250 mL 10% (w/v) aluminium chloride and 250 mL 1 M potassium acetate. The mixture was left at room temperature for 40 min before recording the absorbance at 415 nm. The total flavonol content was measured by mixing 1 mL methanolic extract with 1 mL 2% (w/v) aluminium chloride and 3 mL 5% (w/v) sodium acetate. Then, the absorbance was recorded at 440 nm. Different concentrations of rutin were used as a standard for developing a calibration curve.

ANTIOXIDANT CAPACITY ASSAY BY 2,2-DIPHENYL-1-PICRYLHYDRAZYL (DPPH) RADICAL SCAVENGING

The antioxidant capacity of methanolic extract of the samples was assayed using free radical 2,2-diphenyl-1-picrylhydrazyl (DPPH), as described by Blois (1958). For this purpose, 0.2 mL of methanolic extract was mixed with 1 mL 500 µM DPPH solution. The mixture was vortexed for 30 s and then placed in a dark chamber at room temperature for 30 min. The absorbance was recorded at 517 nm. The antioxidant capacity of the extracts was calculated using the following equation:

$$DPPH\ scavenging\ activity\ (\%) = [(A_{control} - A_{sample}\ (/\ A_{control}] \times 100$$

ASSAY OF COMPATIBLE OSMOLYTES (PROLINE AND GLYCINE BETAINE (GB))

The proline content was determined according to the method of Bates et al. (1973). The fresh leaf samples (0.5 g) were extracted with 5 mL 3% (w/v) sulphosalicylic acid solution. The extracts were centrifuged at 4,000 g for 10 min. Then, 2 mL of the supernatant was mixed with 2 mL ninhydrin solution (1.25 g ninhydrin, 30 mL of acetic acid, and 20 mL of 6 M phosphoric acid) and 2 mL of 96% (v/v) acetic acid. The mixture was incubated at 100°C for 1 h in a hot water bath (model WNB 10, Memmert GmbH, Germany). After incubating, 4 mL of toluene was added to each sample followed by mixing. Eventually, the absorbance of the pink-red upper phase was recorded at 520 nm.

The glycine betaine (GB) content was determined according to the method described by Grieve and Grattan (1983). First, 0.25 g of dried leaf sample was extracted in 10 mL double distilled water and kept at room temperature for

24 h. Then, 250 µL of the extract was filtered and mixed with 250 µL 2 M sulfuric acid in a test tube. The tubes were placed on ice for 1 h. Next, 200 µL cold KI-I_2 reagent (made by dissolving 15.7 g I_2 and 20 g KI in 100 mL distilled water) was added to the tubes and mixed using a vortex mixer (model VX-200, International Inc., Edison, NJ, USA). The tubes were stored in a fridge for 16 h before centrifuging at 10,000 g for 20 min. The pellet (periodide crystals) was dissolved in 9 mL 1,2-dichloroethane and then kept at room temperature for 2 h. Finally, the absorbance was recorded at 365 nm. The GB content (mg g^{-1} DW) was determined using a standard curve.

CARBOHYDRATE (SOLUBLE SUGARS AND STARCH) ASSAY

The phenol-sulfuric acid method was used to measure soluble sugars (Kochert, 1978). The dried and powdered leaf samples (0.1 g) were soaked in 10 mL of 70% (v/v) ethanol for a week at 4°C. Then, 0.5 mL of the solution was mixed with 1.5 mL distilled water and 1 mL of 5% (w/v) phenol. Next, 5 mL of 98% (v/v) sulfuric acid was added and then the samples were placed at room temperature for 30 min to cool down. The absorbance was recorded at 485 nm. The soluble sugar content (mg g^{-1} DW) was determined using a standard glucose curve.

The ethanol-soaked leaf samples from the soluble sugar content test were used to measure the starch content. The samples were filtered through filter paper (Whatman No. 2) and weighted after drying. The samples were placed in test tubes and mixed with 10 mL distilled water and heated on boiling water for 15 min. The samples were filtered again and made up to 25 mL of distilled water. The starch content was measured based on the phenol-sulfuric acid method at 485 nm (Kochert, 1978). The standard curve for soluble sugars was also used to determine the starch content.

SHOOT COBALT CONTENT

The powdered dried shoots (0.5 g) were digested in 5 mL HNO_3 (65% v/v) for 24 h and heated at 90°C for 1 h to digest the tissues. For more digestion, 1 mL H_2O_2 (30% v/v) was added and the samples were placed on a hotplate (LMS-1002, Daihan LabTech, Korea) at 90°C until the mixture dried off. After cooling, their volume was brought to 25 mL with distilled water and cobalt content of the shoot was measured using an inductively coupled plasma optical emission spectrometer (ICP-OES; model SPECTRO ARCOS 76004555, SPECTRO Inc, Kleve, Germany) (Kalra, 1998).

STATISTICAL ANALYSIS

All of the experiments were conducted in a completely randomized design and at least four independent repetitions. Statistical analyses were performed using one-way analysis of variance (ANOVA) by SPSS software, version 22.0 (IBM Corp, Armonk, NY, USA, 2013) and were expressed as the mean values ± SD. The significance of differences between treatments was evaluated using Duncan's test at 5% probability level.

RESULTS AND DISCUSSION

CHARACTERIZATION OF Co_3O_4 NPS

The TEM image exhibited spherical shapes of Co_3O_4 NPs and size as >50 nm (Fig. 1a). According to the AFM measurement, the average size of Co_3O_4 NPs was 50 nm (Fig. 1b–c). DLS results revealed that the hydrodynamic size of cobalt oxide NPs was 26 nm (Fig. 1d). Also, the surface charge (zeta potential) of Co_3O_4 NPs dispersed in deionized water at pH 6.3 was -21.37 mV (Fig. 1e). The structure of Co_3O_4 NPs was investigated using XRD at 2θ angles of 10°-80°) Fig. 1f (The diffraction peaks at 2θ angles: 19.25°, 31.54°, 37.09°, 38.81°, 45.07°, 56.01°, 59.61° and 65.51° corresponded to (111), (220), (311), (222), (400), (422), (511) and (440) planes and were readily indexed to a pure cubic phase structure (JCPDS file no. 01-074-2120) (Fig. 1f).

GROWTH PARAMETERS AND PHOTOSYNTHETIC PIGMENTS

The impacts of Co_3O_4 NPs on the shoot growth characteristics and photosynthetic pigments of canola are presented in Fig. 2. The results indicated that 50 and 100 mg L^{-1} of Co_3O_4 NPs enhanced the shoot length of canola by 12% and 10% compared with the control, respectively (Fig. 2a). Increasing concentration to 500 mg L^{-1} of Co_3O_4 NPs or above resulted in a significant reduction in the shoot length and the minimum one (59%) was related to 4000 mg L^{-1}, compared with the control (Fig. 2a). The fresh weight (FW) of the shoot was enhanced with raising Co_3O_4 NPs concentration up to 100 mg L^{-1} (Fig. 2b). High concentrations of Co_3O_4 NPs led to a significant reduction in the FW of the shoot and the minimum one was obtained when 4000 mg L^{-1} was applied (Fig. 2b). A similar trend was observed in terms of dry weight (DW) of the shoot (Fig. 2c). Application of 50 mg L^{-1} of Co_3O_4 NPs increased the DW of the shoot by 8% compared with the control (Fig. 2c). The minimum DW of the shoot was related to 1000, 2000, and 4000 mg L^{-1} of Co_3O_4 NPs (Fig. 2c).

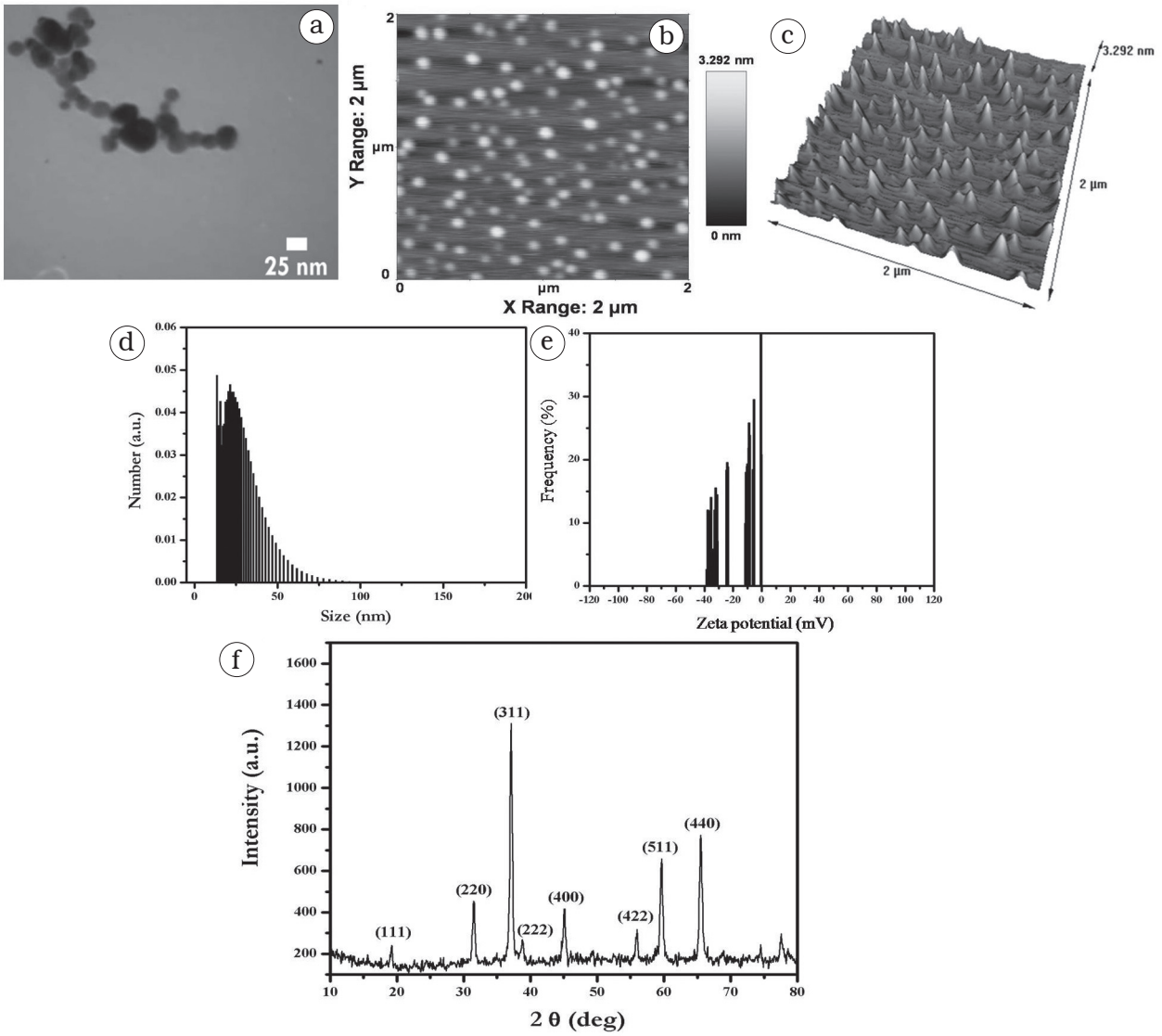

Fig. 1. Images of transmission electron microscopy (TEM; scale bar: 25 nm) (**a**), atomic force microscopy (AFM; scan area: 2 µm × 2 µm) (**b–c**), hydrodynamic diameter (**d**), zeta potential (**e**), and X-ray diffraction (XRD) (**f**) of Co_3O_4 NPs.

In this study, the stimulatory effect of low doses of Co_3O_4 NPs on the shoot growth parameters may be related to the regulation of plant hormone synthesis and activation of enzyme systems determining growth processes. Similarly, the increment in the shoot and root length of *Capsicum chinense* exposed to 100-300 mg L^{-1} of ZnO NPs was reported (Garcia-López et al., 2019). Here, the suppressive effect of high doses of Co_3O_4 NPs on the shoot growth parameters may be due to the heightened levels of ROS and lipoperoxidation. In parallel with the presented results, the diminished FW and DW of maize subjected to 0-1000 mg kg^{-1} nano-Co_3O_4 was demonstrated by Bouguerra et al. (2019).

The results also showed that the content of chlorophyll *a* was increased at 50 and 100 mg L^{-1} of Co_3O_4 NPs but was decreased at high concentrations and the minimum content was at 2000 and 4000 mg L^{-1} (Fig. 2d). A similar trend was observed in chlorophyll *b* and the minimum content was at 4000 mg L^{-1} of Co_3O_4 NPs (Fig. 2d). The total chlorophyll content and chlorophyll *a*/*b* ratio were diminished beyond 250 mg L^{-1} of Co_3O_4 NPs (Fig. 2d-e). The carotenoid content was increased at 50 and 100 mg L^{-1} of Co_3O_4 NPs but was reduced at high concentrations and the minimum one (42% of control) was related to 4000 mg L^{-1} (Fig. 2f).

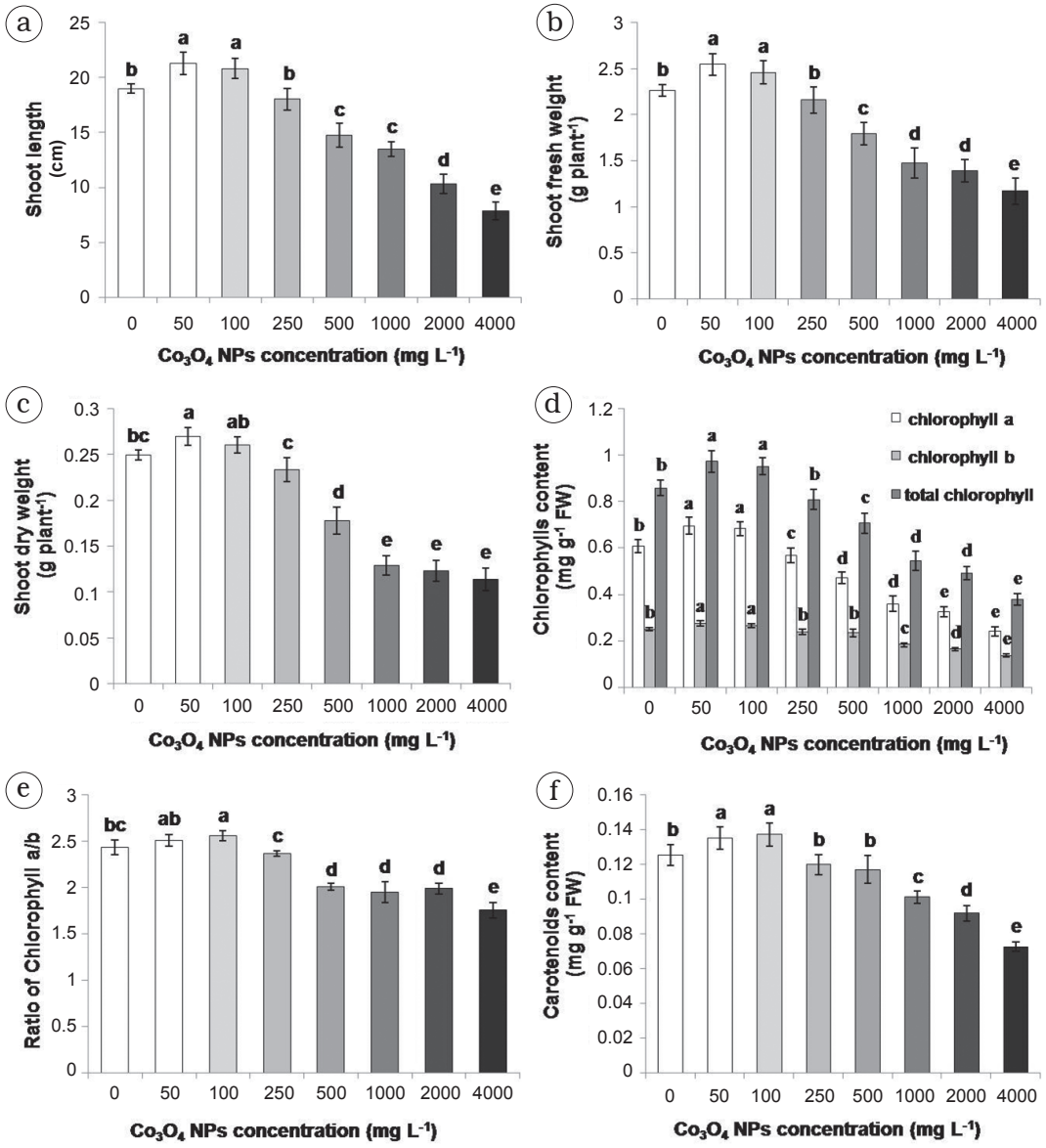

Fig. 2. Effects of spray application of Co_3O_4 NPs on the length (**a**), fresh weight (FW) (**b**), and dry weight (DW) (**c**) of the shoot and the contents of chlorophyll *a*, *b*, and total chlorophyll (**d**), ratio of chlorophyll *a*/*b* (**e**) and carotenoids (**f**) of canola. Means with the same letter do not differ significantly, Duncan's test ($P \leq 0.05$).

It has been reported that NPs of cobalt oxide which is an inorganic catalyst may affect water photo-oxidation and chlorophyll synthesis (Jiao and Frei, 2009; Gopal, 2014). In this study, the enhancement of chlorophyll content at 50 and 100 mg L^{-1} of Co_3O_4 NPs suggested the stimulation of chlorophyll biosynthesis. Similarly, Sonia and Thukral (2014) showed that Co_3O_4 NPs treatment (up to 200 mg kg^{-1}) increased the contents of chlorophyll *a*, *b*, total chlorophyll, and the shoot length of *Hordeum vulgare* but decreased the root length. Also, the increment of carotenoid content in cilantro plants under 100 mg kg^{-1} of ZnO NPs was reported (Reddy Pullagurala et al., 2018). Under different environmental stressors, photosynthesis is affected (Borowiak et al., 2018; Skórska and Murkowski, 2018; Tighe-Neira et al., 2018). Here, reduction of photosynthetic pigments at high concentrations of Co_3O_4 NPs may be attributed to over-production of ROS and damages of photosynthetic apparatus and biomolecules. Therefore, reduction of the chlorophyll value as

well as the inhibition of growth can be regarded as general responses associated with Co_3O_4 NPs toxicity. In parallel with the presented results, López-Luna et al. (2018) reported a considerable decline in photosynthetic pigments in wheat seedling exposed to 500-8000 mg kg^{-1} of nano-cobalt ferrite by free radicals generated by metals.

OXIDATIVE INDICATORS AND SHOOT COBALT CONTENT

The impacts of Co_3O_4 NPs on oxidative indicators and shoot cobalt content in canola are shown in Fig. 3. The results indicated that H_2O_2 content in leaves was increased at 250-4000 mg L^{-1} of Co_3O_4 NPs and the maximum level was recorded at 4000 mg L^{-1} (Fig. 3a). The MDA content in leaves was raised at high concentrations of Co_3O_4 NPs, but no significant difference was observed at 50, 100, and 250 mg L^{-1} (Fig. 3b). The other aldehydes content was elevated beyond 500 mg L^{-1} of Co_3O_4 NPs (Fig. 3c). In the LOX activity, no significant changes were observed by application of Co_3O_4 NPs up to 100 mg L^{-1}, but the activity was increased at higher concentrations (250 to 4000 mg L^{-1}) (Fig. 3d). The MSI was significantly reduced by higher than 250 mg L^{-1} of Co_3O_4 NPs (Fig. 3e).

Oxidative stress occurrs in different plants subjected to NPs. The ROS-induced toxicity may damage the normal physiological redox-regulated functions, which ultimately results in cell death in plants (Meng et al., 2009; Ma et al., 2015). In this study, the concentration-dependent increment of H_2O_2 along with the enhanced antioxidant capacity suggested that the oxidative stress may be the primary mechanism for the toxicity of these NPs, which eventually can lead to cellular damage. Similarly, in rapeseed plants exposed to nano-sized CuO, the heightened H_2O_2 levels, lipoperoxidation and cell death were observed (Nair and Chung, 2017). Also, increment in H_2O_2 levels in radish under 250-2900 mg L^{-1} of Fe_2O_3 NPs was reported (Saquib et al., 2016).

The MDA as an indicator of lipid peroxidation and oxidant state is produced via LOX activity or ROS reactions (Ayala et al., 2014). In this study, the maximum content of MDA was observed at 4000 mg L^{-1} of Co_3O_4 NPs, which may be due to the enhanced LOX activity or the raised values of ROS. Similarly, the increment in H_2O_2 levels, MDA, LOX activity and the decrement in MSI in marigold leaves sprayed with 400-3200 mg L^{-1} of CeO_2 NPs were documented (Jahani et al., 2019).

Here, the heightened ROS levels may damage the cell membrane integrity and MSI, which results in ion leakage and disruption of the cellular metabolism. Singh et al. (2017) reported ion leakage due to the decline of membrane stability in cauliflower and tomato exposed to 50-500 mg L^{-1} of CuO NPs.

The results showed that the shoot cobalt content was linearly raised with increasing Co_3O_4 NPs concentration and the maximum one was observed at 4000 mg L^{-1} (Fig. 3f).

It has been demonstrated that cobalt oxide NPs can cross plasma membranes (Bossi et al., 2016) and plants can absorb and translocate them into different tissues (Amde et al., 2017). The presented results confirmed that in canola plants exposed to foliar application of Co_3O_4 NPs, cobalt was absorbed via the leaves and translocated to the shoots. Similarly, López-Luna et al. (2018) reported accumulation of cobalt and iron in shoots and roots of wheat seedling treated with 500-8000 mg kg^{-1} of nano-cobalt ferrite. Also, foliar Cu accumulation in lettuce and cabbage sprayed with nano-scaled CuO was documented (Xiong et al., 2017). It was reported that different factors such as the NPs characteristics (type, size, dose, surface charge, etc.), plant species, leaf morphology and anatomy, and environmental conditions (light, wind, and moisture) can affect the foliar uptake of NPs (Hong et al., 2014).

NON-ENZYMATIC ANTIOXIDANTS AND ANTIOXIDANT CAPACITY

The impacts of Co_3O_4 NPs on non-enzymatic antioxidants and antioxidant capacity of canola leaves are presented in Fig. 4. The results showed that the application of high concentrations of Co_3O_4 NPs diminished the ASC content and ASC/DHA ratio but increased the DHA content (Fig. 4a–c). Application of Co_3O_4 NPs at dosages less than 1000 mg L^{-1} did not show any significant impact on the GSH content but decreased it at higher concentrations (Fig. 4d). The contents of total flavonoids and flavonols were elevated after application of 1000 and 2000 mg L^{-1} of Co_3O_4 NPs, respectively (Fig. 4e–f).

Plants have evolved an antioxidant defence mechanism as the first line of defence, which involves enzymatic and non-enzymatic components to minimize the oxidative damage during exposure to metal oxide-based NPs (Ma et al., 2015).

It has been reported that cobalt NPs can cause oxidative loss of ASC in cells and biological fluids (Salnikow et al., 2004). The presented results indicated that increase of Co_3O_4 NPs induced oxidative stress and led to decrease in the ASC content, whereas DHA was raised.

GSH is known as the most important defence against ROS in plants exposed to metal stress (Hasanuzzaman et al., 2017). However, during strong stresses, degradation of the GSH pool may occur (Hernández et al., 2015). In this study, the decrease of GSH content at high concentrations of

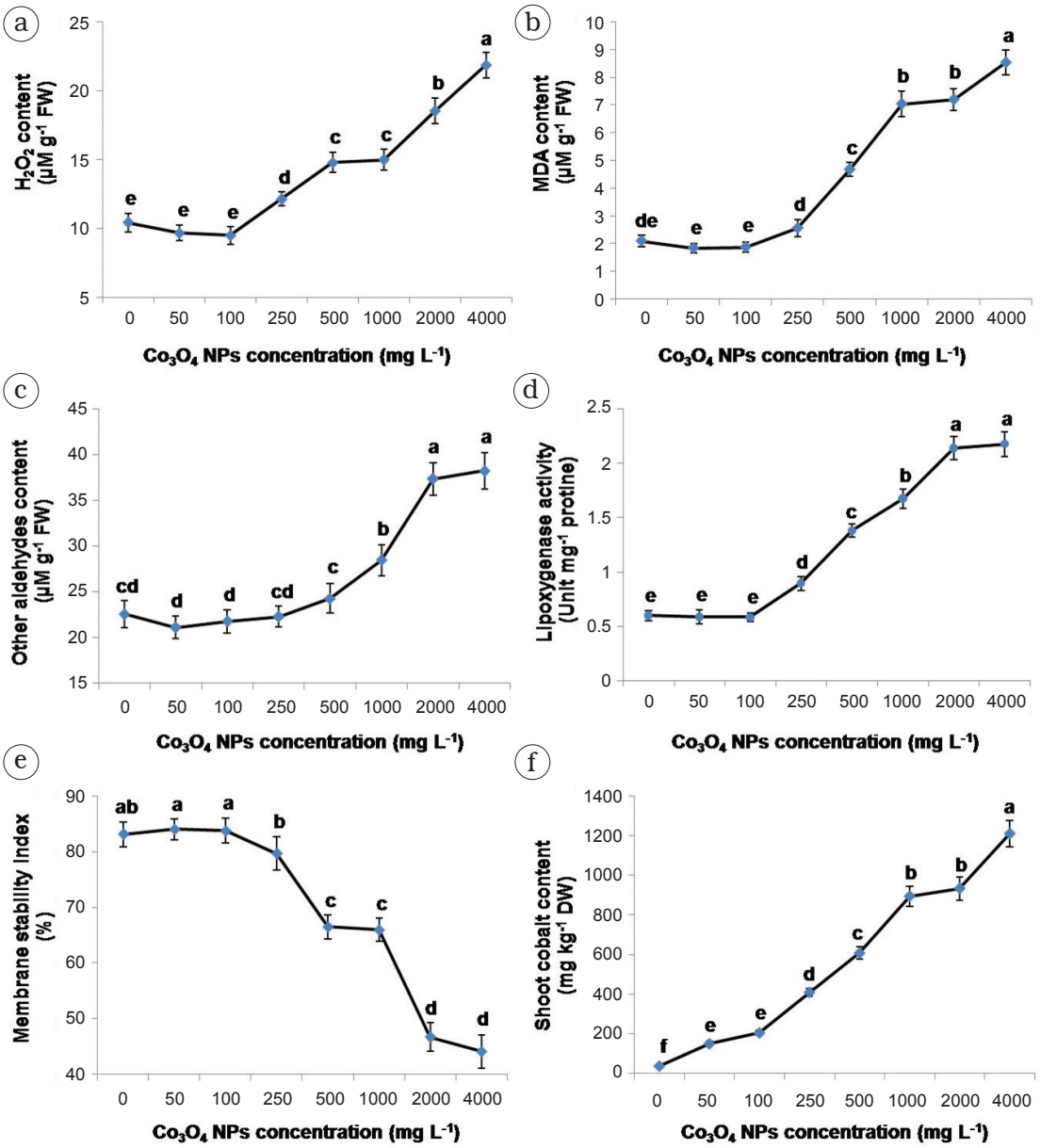

Fig. 3. Effects of spray application of Co_3O_4 NPs on the contents of H_2O_2 (**a**), malondialdehyde (MDA) (**b**), other aldehydes (**c**) lipoxygenase (LOX) enzyme activity (**d**), membrane stability index (MSI) (**e**), and shoot cobalt accumulation (**f**) of canola. Means within a column with the same letter do not differ significantly, Duncan's test ($P \leq 0.05$).

Co_3O_4 NPs was observed. Similarly, the usage of 200 µM of cerium heightened the DHA level and lowered GSH and the proportion of DHA/total ASC in *Oryza sativa* seedlings (Xu and Chen, 2011). Furthermore, the lowered level of GSH in *Arabidopsis* subjected to 5.8 µM quantum dot NPs was observed (Navarro et al., 2012). In contrast, the incremented ASC in rice under 2.5–1000 mg L^{-1} of nano-scaled CuO was reported (Da Costa and Sharma, 2016). In this study, the declined levels of ASC and GSH and the raised levels of DHA may be due to ROS accumulation, which may cause the interruption in ASC-GSH cycle and the decline in ASC and GSH recovery.

Flavonoids as non-enzymatic antioxidant components participate in neutralizing of free radicals (Skórska et al., 2019). In this study, the enhancement of flavonoid and flavonol contents

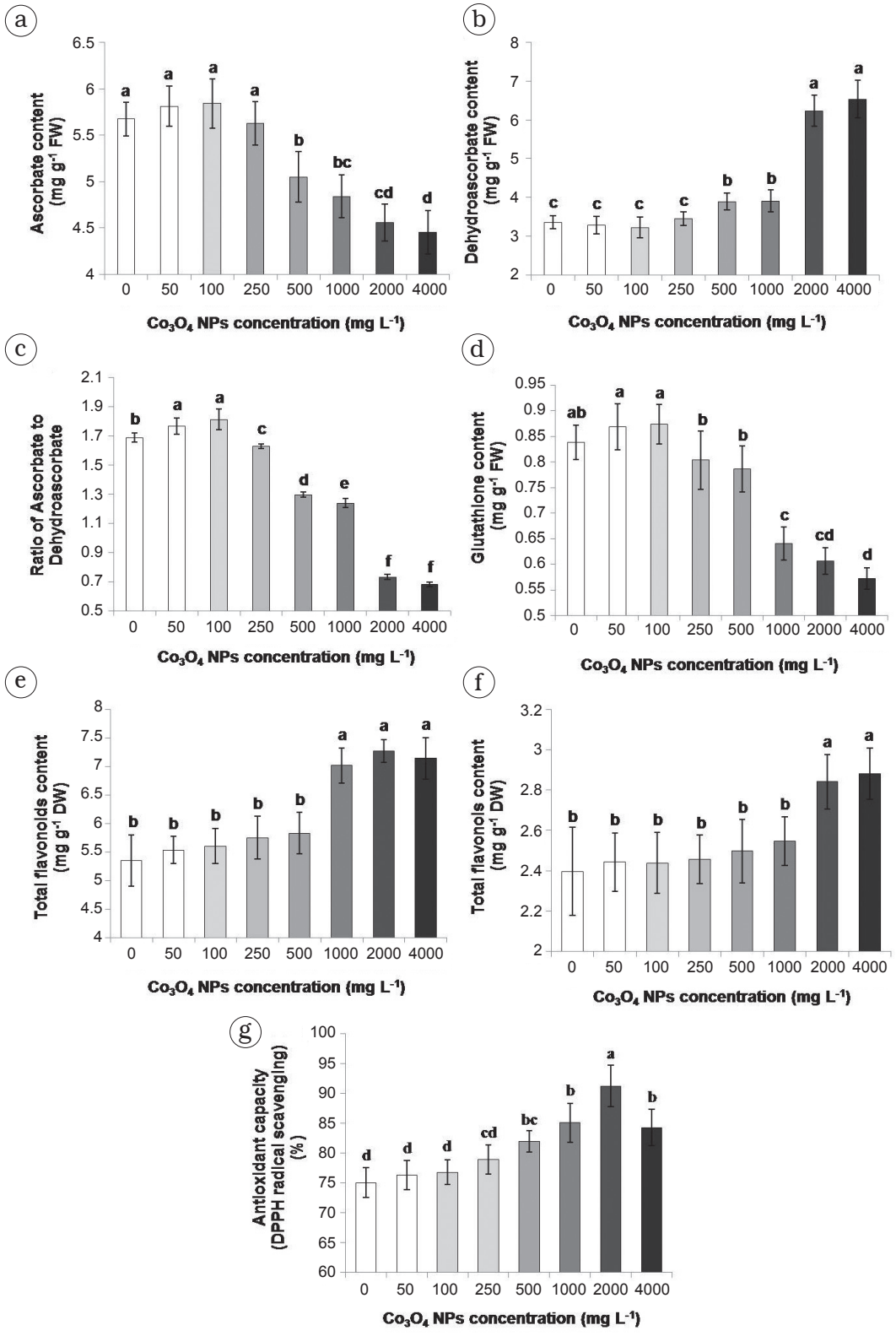

Fig. 4. Effects of spray application of Co_3O_4 NPs on the contents of ascorbate (ASC) (**a**), dehydroascorbate (DHA) (**b**), ASC/DHA ratio (**c**), glutathione (GSH) (**d**), total flavonoids (**e**), flavonols (**f**), and antioxidant capacity (DPPH) (**g**) of canola leaves. Means with the same letter do not differ significantly, Duncan's test ($P \leq 0.05$).

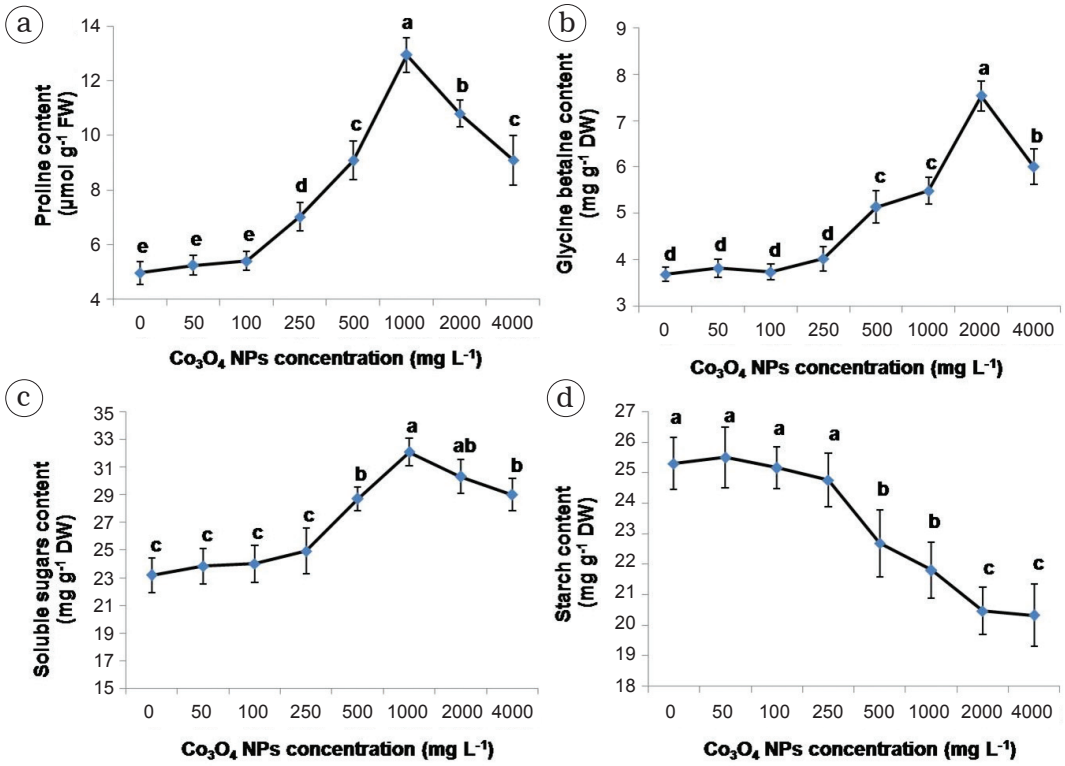

Fig. 5. Effects of spray application of Co_3O_4 NPs on the contents of proline (**a**), glycine betaine (GB) (**b**), soluble sugars (**c**), and starch (**d**) of canola leaves. Means within a column with the same letter do not differ significantly, Duncan's test ($P \leq 0.05$).

may protect the cellular components from damages of oxidative stress caused by NPs. These observations were congruent with the findings of Zafar et al. (2016) on *Brassica nigra* subjected to 500–1500 mg L^{-1} of CuO NPs. Also, the incremented levels of total flavonoids in eggplant (*Solanum melongena*) exposed to three different NPs (ZnO, NiO and CuO) were demonstrated (Baskar et al., 2018).

The results showed that the antioxidant capacity was increased with higher concentrations (500–2000 mg L^{-1}) of Co_3O_4 NPs but was diminished at 4000 mg L^{-1} (Fig. 4g). Similarly, Mohsenzadeh and Moosavian (2017) demonstrated the increment in antioxidant capacity in rosemary (*Rosmarinus officinalis*) leaves subjected to nano-scales ZnO NPs.

COMPATIBLE OSMOLYTES AND CARBOHYDRATE CONTENTS

The impacts of Co_3O_4 NPs on compatible osmolytes and carbohydrate contents of canola are presented in Fig. 5. The results showed that the content of proline was elevated upon usage of Co_3O_4 NPs up to 1000 mg L^{-1}, but it was decreased at higher concentrations (Fig. 5a). A similar trend was observed in GB content and the maximum one was related to 2000 mg L^{-1} of Co_3O_4 NPs (Fig. 5b).

Proline and GB as compatible osmolytes protect plants under environmental stresses (Singh et al., 2015). In this study, the increased levels of proline and GB in response to high concentrations of Co_3O_4 NPs could be a biochemical adaptation to scavenge ROS. Similarly, in rice, the increment of the proline level due to the usage of 1000 mg L^{-1} of nano scaled-CuO was reported (Da Costa and Sharma, 2016). Also, the raised proline content in wheat subjected to 25–50 mg mL^{-1} of nano-sized Al_2O_3 was observed (Yanik and Vardar, 2018).

The results showed that high concentrations of Co_3O_4 NPs increased the soluble sugar content in leaves and reached the maximum value (38% of control) at 1000 mg L^{-1} (Fig. 5c). The starch content was stable up to 250 mg L^{-1} of Co_3O_4 NPs, but it was reduced at higher concentrations. The minimum starch value was observed when 2000 or 4000 mg L^{-1} of Co_3O_4 NPs were applied (Fig. 5d).

Carbohydrates have several functions in plants, ranging from energy storage to signalling

and plant adaptation in environmental stresses (Sami et al., 2016). In this study, reduction of starch and accumulation of soluble sugars as possible oxidative stress indicators could provide energy and solutes for osmotic adjustment at high concentrations of Co_3O_4 NPs. Similarly, nano-scaled CuO (50–200 mg kg^{-1}) diminished the starch value in oregano (*Origanum vulgare*) leaves (Du et al., 2018). In another study, the increase of soluble sugars in rosemary leaves subjected to 4000 and 7000 mg L^{-1} of nano-sized ZnO was reported (Mohsenzadeh and Moosavian, 2017). Also, the increment of soluble sugars in wheat subjected to 1500 mg L^{-1} of nano Zn and Fe oxide was demonstrated (Babaei et al., 2017).

Overall, canola showed a dual response to different concentrations of Co_3O_4 NPs. Canola growth and photosynthesis were stimulated at low concentrations of Co_3O_4 NPs, whereas canola was susceptible to high concentrations of Co_3O_4 NPs despite the activated defence and osmoregulating system and eventually it showed phytotoxicity symptoms of Co_3O_4 NPs. In addition, a schematic image of the present study is displayed in Supplementary Fig. S2.

CONCLUSION

Nowadays, the beneficial and toxic impacts of Co_3O_4 NPs in plants are still in its infancy and have remained largely unexplored. In this study, the impact of Co_3O_4 NPs on canola was concentration-dependent. In most cases, lower concentrations of Co_3O_4 NPs (50 and 100 mg L^{-1}) had positive or no significant effects on morpho-physiological or biochemical parameters. Despite the accumulation of non-enzymatic antioxidants and compatible osmolytes, toxic effects of high concentrations of Co_3O_4 NPs may interfere with plant functions and cause physiological damages such as lipid peroxidation and cell membrane instability. It can be concluded that the plant defence strategy did not have enough efficiency to endure Co_3O_4 NPs toxicity. The results suggested the necessity of phytotoxicity studies of Co_3O_4 NPs to understand their functional mechanisms in other crop plants.

AUTHORS' CONTRIBUTIONS

The present study was accomplished with the collaboration of all authors. M.J. performed the experiments, analyzed the data and wrote the first draft of the manuscript; RA.K-N. and S.S. designed the experiment, wrote the protocol and checked the manuscript; H.M. designed a part of experiments and checked the manuscript. The authors declare that they have no conflicts of interest.

ACKNOWLEDGMENTS

This work is as a part of Ph.D. thesis of M.J. and the authors are grateful to Roksana Pesian and Fatemeh Khakrah in Central Lab of the Ferdowsi University of Mashhad, Iran for their technical help in assays of characteristics of Co_3O_4 NPs. This research did not receive any specific grant from funding agencies in the public, commercial, or not-for-profit sectors.

REFERENCES

Akkol Ek, Goger F, Kosar M, and Baser HC. 2008. Phenolic composition and biological activities of *Salvia halophila* and *Salvia virgata* from Turkey. *Food Chemistry* 108: 942–949.

Amde M, Liu Jf, Tan ZQ, and Bekana D. 2017. Transformation and bioavailability of metal oxide nanoparticles in aquatic and terrestrial environments. A review. *Environmental pollution* 230: 250–267.

Ayala A, Muñoz MF, and Argüelles S. 2014. Lipid peroxidation: production, metabolism, and signaling mechanisms of malondialdehyde and 4-hydroxy-2-nonenal. *Oxidative Medicine and Cellular Longevity* 2014: 31. https://doi.org/10.1155/2014/360438.

Babaei K, Seyed Sharifi R, Pirzad A, and Khalilzadeh R. 2017. Effects of bio fertilizer and nano Zn-Fe oxide on physiological traits, antioxidant enzymes activity and yield of wheat (*Triticum aestivum* L.) under salinity stress. *Journal of Plant Interaction* 12(1): 381–389.

Barceloux DG, and Barceloux D. 1999. Cobalt. *Journal of Toxicology: Clinical Toxicology* 37(2): 201–216.

Baskar V, Nayeem S, Kuppuraj Sp, Muthu T, and Ramalingam S. 2018. Assessment of the effects of metal oxide nanoparticles on the growth, physiology and metabolic responses in *in vitro* grown eggplant (*Solanum melongena*). *3 Biotech* 8(8): 362.

Bates Ls, Waldren RP, and Teare ID. 1973. Rapid determination of free proline for water-stress studies. *Plant Soil* 39(1): 205–207.

Blois MS. 1958. Antioxidant determinations by the use of a stable free radical. *Nature* 181: 1199–1200.

Borowiak K, Budka A, Hanć A, Kayzer D, Lisiak M, Zbierska J, Baralkiewicz D, Iwaniuk D, and Łopatka N. 2018. Relations between photosynthetic pigments, macro-element contents and selected trace elements accumulated in *Lolium multiflorum* L. exposed to ambient air conditions. *Acta Biologica Cracoviensia Series Botanica* 60(1): 35–44.

Bossi E, Zanella D, Gornati R, and Bernardini G. 2016. Cobalt oxide nanoparticles can enter inside the cells by crossing plasma membranes. *Nature Scientific Reports* 6: 22254.

Bouguerra S, Gavina A, Da Graca Rasteiro M, Rocha-Santos T, Ksibi M, and Pereira R. 2019. Effects of cobalt oxide nanomaterial on plants and soil invertebrates at different levels of biological organization. *Journal of Soils and Sediments*. https://doi.org/10.1007/s11368-019-02285-8.

Cui D, Zhang P, Ma Y, He X, Li Y, Zhang J, Zhao Y, and Zhang Z. 2014. Effect of cerium oxide nanoparticles on asparagus

lettuce cultured in an agar medium. *Environmental Science: Nano* 1: 459–465.

Da Costa MVJ, and Sharma PK. 2016. Effect of copper oxide nanoparticles on growth, morphology, photosynthesis, and antioxidant response in *Oryza sativa*. *Photosynthetica* 54(1): 110–119.

De Pinto Mc, Francis D, and De Gara L. 1999. The redox state of the ascorbate-dehydroascorbate pair as a specific sensor of cell division in tobacco BY-2 cells. *Protoplasma* 209: 90–97.

Doderer A, Kokkelink I, Van Der Veen S, Valk B, Schram AW, and Douma AC. 1992. Purification and characterization of two lipoxygenase isoenzymes from germinating barley. *Biochimica et Biophysica Acta* 1120: 97–104.

Du W, Tan W, Yin Y, Ji R, Peralta-Videa Jr, Guo H, and Gardea-Torresdey JL. 2018. Differential effects of copper nanoparticles/microparticles in agronomic and physiological parameters of oregano (*Origanum vulgare*). *Science of the Total Environment* 618: 306–312.

Ellman GL. 1959. Tissue sulfydryl groups. *Archives of Biochemistry and Biophysics* 82: 70–77.

Faisal Mi, Saquib Q, Alatar Aa, Al-Khedhairy Aa, Ahmed M, Ansari Sm, Alwathnani Ha, Dwivedi S, Musarrat J, and Praveen S. 2016. Cobalt oxide nanoparticles aggravate DNA damage and cell death in eggplant via mitochondrial swelling and NO signaling pathway. *Biological Research* 49(20): 1–13.

Garcia-López Ji, Lira-Saldivar Rh, Zavala-Garcia F, Olivares-Saenz E, Nino-Medina G, Ruiz-Torres Na, Mendez-Arguello B, and Diaz-Barriga E. 2019. Effects of zinc oxide nanoparticles on growth and antioxidant enzymes of *Capsicum chinense*. *Toxicological and Environmental Chemistry*. https://doi.org/10.1080/02772248.2018.1550781.

Ghodake G, Seo YD, and Lee DS. 2011. Hazardous phytotoxic nature of cobalt and zinc oxide nanoparticles assessed using *Allium cepa*. *Journal of Hazardous Materials* 186: 952–955.

Gopal R. 2014. Antioxidant defense mechanism in pigeon pea under cobalt stress. *Journal of Plant Nutrition* 37(1): 136–145.

Grieve CM, and Grattan SR. 1983. Rapid assay for determination of water soluble quaternary amino compounds. *Plant Soil* 70: 303–307.

Hasanuzzaman M, Nahar K, Anee TI, and Fujita M. 2017. Glutathione in plants: biosynthesis and physiological role in environmental stress tolerance. *Physiology and Molecular Biology of Plants* 23(2): 249–268.

Heath RL, and Packer L. 1968. Photoperoxidation in isolated chloroplasts kinetics and stoichiometry of fatty acid peroxidation. *Archives of Biochemistry and Biophysics* 125: 189–198.

Hernández Le, Sobrino-Plata J, Montero-Palmero Mb, Carrasco-Gil S, Flores-Cáceres Ml, Ortega-Villasante C, and Escobar C. 2015. Contribution of glutathione to the control of cellular redox homeostasis under toxic metal and metalloid stress. *Journal of Experimental Botany* 66(10): 2901–2911.

Hong J, Peralta-Videa Jr, Rico C, Sahi S, Viveros Mn, Bartonjo J, Zhao L, and Gardea-Torresey JL. 2014. Evidence of translocation and physiological impacts of foliar applied CeO_2 nanoparticles on cucumber (*Cucumis sativus*) plants. *Environmental Science and Technology* 48: 4376–4385.

Jahani S, Saadatmand S, Mahmoodzadeh H, and Khavari-Nejad RA. 2019. Effects of cerium oxide nanoparticles on biochemical and oxidative parameters in marigold leaves. *Toxicological and Environmental Chemistry*. https://doi.org/10.1080/02772248.2019.1587443.

Janmohammadi M, Yousefzadeh S, Dashti S, and Sabaghnia N. 2017. Effects of exogenous application of nano particles and compatible organic solutes on sunflower (*Helianthus annuus* L.). *Botanica Serbica* 41(1): 37–46.

Jiao F, and Frei H. 2009. Nanostructured cobalt oxide clusters in mesoporous silica as efficient oxygen-evolving catalysts. *Angewandte Chemie International Edition in English* 48(10): 1841–1844.

Kalra YP. 1998. *Handbook of reference methods for plant analysis*. CRC Press, Boca Raton, FL.

Kochert G. 1978. Carbohydrate determination by the phenol-sulfuric acid method. In: Hellebust JA, Craigie JS [eds.], *Handbook of Phycological Methods: Physiological and Biochemical Methods*, 95–97. Cambridge University Press, Cambridge.

Lichtenthaler HK. 1987. Chlorophylls and carotenoids: pigments of photosynthetic biomembranes. *Methods in Enzymology* 148: 350–382.

Lin L, Allemekinders H, Dansby A, Campbell L, Durance-Tod S, Berger A, and Jones PJ. 2013. Evidence of health benefits of canola oil. *Nutrition Reviews* 71(6): 370–385.

Loganes C, Ballali S, and Minto C. 2016. Main properties of canola oil components: a descriptive review of current knowledge. *The Open Agriculture Journal* 10: 69–74.

López-Luna J, Camacho-Martínez Mm, Solís-Domínguez Fa, González-Chávez Mc, Carrillo-González R, Martinez-Vargas S, Mijangos-Ricardez OF, and Cuevas-Díaz MC. 2018. Toxicity assessment of cobalt ferrite nanoparticles on wheat plants. *Journal of Toxicology and Environmental Health, Part A* 81(14): 604–619.

Ma C, White Jc, Dhankher OP, and Xing B. 2015. Metal-based nanotoxicity and detoxification pathways in higher plants. *Environmental Science and Technology* 49 (12): 7109–7122.

Meng H, Xia T, George S, and Nel AE. 2009. A predictive toxicological paradigm for the safety assessment of nanomaterials. *ACS Nano* 3(7): 1620–1627.

Miers S, Philosoph-Hadas S, and Aharoni N. 1992. Ethylene induced accumulation of lipid products fluorescent during senescence of parsley by a newly developed method. *Journal of the American Society for Horticultural Science* 117: 128–132.

Mohsenzadeh S, and Moosavian SS. 2017. Zinc sulphate and nano-zinc oxide effects on some physiological parameters of *Rosmarinus officinalis*. *American Journal of Plant Sciences* 8(11): 2635–2649.

Nair PMG, and Chung IM. 2017. Evaluation of stress effects of copper oxide nanoparticles in *Brassica napus* L. seedlings. *3 Biotech* 7: 293.

Navarro Da, Bisson MA, and Aga DS. 2012. Investigating uptake of water-dispersible CdSe/ZnS quantum dot nanoparticles by *Arabidopsis thaliana* plants. *Journal of Hazardous Materials* 211–212: 427–435.

Ngo Qb, Dao Th, Nguyen Hc, Tran Xt, Nguyen Tv, Khuu TD, and Huynh TH. 2014. Effects of nanocrystalline powders (Fe, Co and Cu) on the germination, growth, crop yield and product quality of soybean (Vietnamese species DT-51).

Advances in Natural Sciences: Nanoscience and Nanotechnology 5(1): 015016 (7pp).

Rastogi A, Zivcak M, Sytar O, Kalaji Hm, He X, Mbarki S, and Brestic M. 2017. Impact of metal and metal oxide nanoparticles on plant: a critical review. *Frontiers in Chemistry* 5: 78.

Reddy Pullagurala Vl, Adisa Io, Rawat S, Kalagara S, Hernandez-Viezcas Ja, Peralta-Videa JR, and Gardea-Torresdey JL. 2018. ZnO nanoparticles increase photosynthetic pigments and decrease lipid peroxidation in soil grown cilantro (*Coriandrum sativum*). *Plant Physiology and Biochemistry* 132: 120–127.

Sairam Rk, Deshmukh PS, and Shukla DS. 1997. Tolerance to drought and temperature stress is a relation to increased antioxidant enzyme activity in wheat. *Journal of Agronomy and Crop Science* 178: 171–177.

Salnikow K, Donald Sp, Bruick Rk, Zhitkovich A, Phang JM, and Kasprzak KS. 2004. Depletion of intracellular ascorbate by the carcinogenic metals nickel and cobalt results in the induction of hypoxic stress. *Journal of Biological Chemistry* 279(39): 40337–40344.

Sami F, Yusuf M, Faizan M, Faraz A, and Hayat S. 2016. Role of sugars under abiotic stress. *Plant Physiology and Biochemistry* 109: 54–61.

Saquib Q, Faisal M, Alatar Aa, Al-Khedhairy Aa, Ahmed M, Ansari Sm, Alwathnani Ha, Okla Mk, Dwivedi S, Musarrat J, Praveen S, Khan St, Wahab R, Siddiqui MA, and Ahmad J. 2016. Genotoxicity of ferric oxide nanoparticles in *Raphanus sativus*: deciphering the role of signaling factors, oxidative stress and cell death. *Journal of Environmental Sciences* 47: 49–62.

Singh A, Singh Nb, Hussain I, and Singh H. 2017. Effect of biologically synthesized copper oxide nanoparticles on metabolism and antioxidant activity to the crop plants *Solanum lycopersicum* and *Brassica oleracea* var. *botrytis*. *Journal of Biotechnology* 262: 11–27.

Singh M, Kumar J, Singh S, and Prasad SM. 2015. Roles of osmoprotectants in improving salinity and drought tolerance in plants: a review. *Reviews in Environmental Science and Bio/Technology* 14(3): 407–426.

Skórska E, and murkowski A. 2018. Photosynthetic responses of *Chlorella vulgaris* L. to short-term UV-B radiation exposure. *Acta Biologica Cracoviensia Series Botanica* 60(1): 65–71.

Skórska E, Grzeszczuk M, Barańska M, and Wójcik-Stopczyńska B. 2019. Long wave UV-B radiation and Asahi SL modify flavonoid content and radical scavenging activity of *Zea mays* var. *saccharata* leaves. *Acta Biologica Cracoviensia Series Botanica* 61(1): 87–92.

Sonia, and Thukral AK. 2014. Effects of macro- and nano-cobalt oxide particles on barley seedlings and remediation of cobalt chloride toxicity using sodium hypochlorite. *International Journal of Plant and Soil Science* 3(6): 751–762.

Srivastava N. 2015. Interaction of cobalt nanoparticles with plants: a cytogenetical aspect. *Journal of Experimental Nanoscience* 10(10): 769–776.

Tighe-Neira R, Carmora E, Recio G, Nunes-Nesi A, Reyes-Diaz M, Alberdi M, Rengel Z, and Inostroza-Blancheteau C. 2018. Metallic nanoparticles influence the structure and function of the photosynthetic apparatus in plants. *Plant Physiology and Biochemistry* 130: 408–417.

Velikova V, Yordanov I, and Edreva A. 2000. Oxidative stress and some antioxidant systems in acid rain-treated bean plants: protective role of exogenous polyamines. *Plant Science* 151(1): 59-66.

Wu Sg, Huang L, Head J, Chen Dr, Kong IC, and Tang YJ. 2012. Phytotoxicity of metal oxide nanoparticles is related to both dissolved metals ions and adsorption of particles on seed surfaces. *Journal of Petroleum and Environmental Biotechnology* 3: 126. doi:10.4172/2157-7463.1000126.

Xiong Tt, Dumat C, Dappe V, Vezin H, Schreck E, Shahid M, Pierart A, and Sobanska S. 2017. Copper oxide nanoparticle foliar uptake, phytotoxicity, and consequences for sustainable urban agriculture. *Environmental Science and Technology* 51(9): 5242–5251.

Xu QM, and Chen H. 2011. Antioxidant responses of rice seedling to Ce^{4+} under hydroponic cultures. *Ecotoxicology and Environmental Safety* 74: 1693–1699.

Yanik F, and Vardar F. 2018. Oxidative stress response to aluminum oxide (Al_2O_3) nanoparticles in *Triticum aestivum*. *Biologia* 73: 129–135.

Zafar H, Ali A, and Zia M. 2016. CuO nanoparticles inhibited root growth from *Brassica nigra* seedlings but induced root from stem and leaf explants. *Applied Biochemistry and Biotechnology* 181(1): 365–378.